Performance Study of Statistical and Deterministic Channel Models for mmWave Wi-Fi Networks in ns-3

Yuchen Liu, Shelby K. Crisp, Douglas M. Blough
Georgia Institute of Technology
Atlanta, Georgia, USA
{yuchen.liu,scrisp3}@gatech.edu, doug.blough@ece.gatech.edu

ABSTRACT

To address the needs of emerging bandwidth-intensive applications in 5G and beyond era, the millimeter-wave (mmWave) band with very large spectrum availability have been recognized as a promising choice for future wireless communications. In particular, IEEE 802.11ad/ay operating on 60 GHz carrier frequency is a highly anticipated wireless local area network (WLAN) technology for supporting ultra-high-rate data transmissions. In this paper, we describe additions to the ns-3 802.11ad simulator that include 3-D obstacle specifications, line-of-sight calculations, and a sparse cluster-based channel model, which allow researchers to study complex mmWave Wi-Fi network deployments under more realistic conditions. We also study the performance accuracy and simulation efficiency of the implemented statistical channel model as compared to a deterministic ray-tracing based channel model. Through extensive ns-3 simulations, the results show that the implemented channel model has the potential to achieve good accuracy in performance evaluation while improving simulation efficiency. We also provide a detailed parametric analysis on the statistical channel model, which yields insight on how to properly tune the model parameters to further improve performance accuracy.

CCS CONCEPTS

• **Networks** → **Network simulations**; **Network performance analysis**; **Mobile network**.

KEYWORDS

ns-3, millimeter wave, simulation, Wi-Fi, 802.11ad, sparse cluster-based channel model, ray tracing.

1 INTRODUCTION

In 5G and 6G eras, the proliferation of mobile devices with data hungry applications, such as virtual/augmented reality and real-time high-definition video, is pushing communication to higher carrier frequencies, e.g. the mmWave band, which has a very large amount of bandwidth available. In recent years, several standardization efforts such as IEEE 802.11ad/ay [7, 8] and Wireless Gigabit Alliance (WiGig) are tailored to enable 60 GHz mmWave communication for wireless local-area networks (WLANs) to support the emerging bandwidth-intensive applications.

However, 60 GHz radios are extremely vulnerable to propagation loss and blockage effects [12], which makes the network performance quite sensitive to environmental characteristics. In this regard, an accurate and reliable performance evaluation of such complex network becomes critical to identify which protocols and network deployments can provide the best quality of experience to the end user. Network simulation plays a significant role in testing the next-generation network performance by allowing researchers to better explore the space of networking solutions through extensive variation of the network configuration parameters and environment settings. In particular, ns-3 [16] is a powerful system-level simulation tool for evaluating wireless networks, where a number of advanced features have been developed and integrated, such as mmWave and NR modules [19] for cellular networks, and extended Wi-Fi modules to support IEEE 802.11ad/ax/ay [2, 9] for WLANs.

For end-to-end 802.11ad/ay WLAN simulations, an accurate channel model, which takes into account important properties of 60 GHz electromagnetic waves propagation and environment features, is of paramount importance to assess the system design and performance. Different from the propagation characteristics at frequency bands below 6 GHz, the diffraction ability of mmWave signal is much weaker and less reliable due to its smaller wavelength. In particular, obstacles blocking the line-of-sight transmission path create a much more substantial problem for mmWave signals. While objects in the environment can act as scatterers or reflectors to create alternative links, the quality is highly dependent on the environmental characteristics, e.g., geometrical layout and object reflectivity.

In traditional WLANs operating on the carrier frequency of 2.4 or 5 GHz, the channel modeling approach generates separate models for path loss and channel impulse response (CIR) since most of the channel paths contribute to the total received signal power. Thus, the path loss function (e.g., in log-distance based channel model) can well describe average power behavior of electromagnetic field for different distances. However, in WLANs operating in the mmWave band, the use of highly directional antennas and its multi-path sparsity nature will filter out all but a few clusters of

the propagation channel, where both the frequency selectivity and propagation loss of the channel is defined by the characteristics of the clusters. Thus, the path loss and CIR may be significantly different depending on the characteristics of each cluster, and the simple path-loss model is no longer able to accurately describe the channel characteristics. Therefore, for the design and simulation of mmWave WLANs, it is necessary to account for the space and time of the multi-path components (MPCs) to accurately model the channel. To this end, statistical modeling and deterministic modeling are the two most popular approaches. Statistical channel models generate the MPCs from a set of random probabilistic distributions, whose parameters are determined by a statistically fit from actual channel measurement data. Deterministic channel models rely on ray tracing to characterize the explicit propagation properties of every path component using geometrical optics, which provides an extremely precise channel characteristic when the environment details are known.

In this paper, we conduct a comprehensive performance study on a statistical channel model and a deterministic ray-tracing based channel model in mmWave Wi-Fi networks using ns-3. We first develop an obstacle-specific scenario module and a sparse cluster-based channel module in ns-3, which accurately model obstacles and build environment features into the propagation model. Then, through extensive network simulations, we study the performance accuracy and simulation efficiency of the implemented statistical channel model by using a ray-tracing based channel model as the comparison point. The main contributions of this work are as follows:

- We develop an obstacle-specific scenario model in ns-3, which allows the user to flexibly simulate various mmWave WLAN scenarios with actual object deployment and accurate LoS determination.
- We implement a sparse cluster-based (SC) wireless channel model in ns-3 that statistically models multi-path components in 802.11ad/ay enabled Wi-Fi networks.
- We perform a detailed comparison between the statistical channel model and ray-tracing based channel model, where the results show that the implemented SC channel model has potential to achieve an acceptable accuracy in performance evaluation while maintaining a good simulation efficiency.
- We conduct a parametric analysis on SC channel model, which yields insight on how to properly tune the modeling parameters to further improve the performance accuracy.

2 OVERVIEW OF CHANNEL MODELING FOR MMWAVE NETWORKS

Channel modeling is critical to evaluate the performance of next-generation wireless network, here we give an overview of different channel models used in mmWave networks.

2.1 Log-distance Based Model

The log-distance-based propagation model is widely used in wireless networks, where the propagation loss between transmitter and receiver is calculated based on a simple path loss model, i.e. a closed-form formula that depends on the signal frequency and separation distance. Then, based on the actual measurement in the

environment, some modeling parameters (e.g., path loss exponent α) are tuned to make the path-loss calculation fit the actual measurement data as much as possible. For example, [22] evaluated a generic indoor path-loss model in the 60 GHz band for the LoS and non-LoS (NLoS) cases in a laboratory scenario, where the path-loss exponents were measured as 2.0 and 5.4, respectively. In the technical report of 3GPP [1], multiple path loss models are defined to apply in different scenarios, including outdoor urban/rural scenario and indoor scenario, where the specified expression and standard deviation of multi-path fading distribution are also given for each scenario. However, as communication moves to higher frequencies, e.g., mmWaves, this kind of channel model becomes highly inaccurate, especially in NLoS scenarios since it fails to capture the explicit multi-path components (MPCs) of the signal.

2.2 Statistical Model

The statistical model describes the stochastic characteristic of amplitudes of the resolvable MPCs and path time of arrival in a wireless network. MPCs are clustered in both spatial and temporal domains, where a cluster consists of a group of rays having similar delays and directions of departure and arrival. Actual measurement data is used to statistically characterize the inter-cluster and intra-cluster properties in propagation channel. A popular and widely-used statistical model is the Saleh-Valenzuela (S-V) channel model [20], where clusters and rays are modeled with specific probability distributions. In recent years, a number of works studied the use of this cluster-based channel model in mmWave networks [21, 23, 24]. For example, [23] studied a 60 GHz channel model for indoor office environment based on the S-V model with spatio-temporal clustering properties. [21] proposed a S-V model that is useful in designing mmWave WPAN systems used in a conference room environment. The S-V model is an example of a sparse cluster-based (SC) channel model, because it is tailored to the narrow-beam directional antennas and limited scattering nature of mmWave wireless networks.

The statistical nature of these models makes them more easily model common indoor office/lab scenarios and effectively reproduce the stochastic properties of mmWave channels in a given type of environment, but may prevent researchers from evaluating the impact of the channel dynamics in a specific environment or site.

2.3 Ray-tracing Based Model

Ray tracing techniques can be used to precisely model the propagation of mmWave signals in any specific scenario [5, 10]. Different from statistical channel models, the cluster and ray found using ray tracing technology is based on the geometry of scenario and physical interaction with the environment, which can characterize the explicit propagation properties of each MPC, including angle of arrival at the receiver, angle of departure at the transmitter, time delay, path gain, doppler shift, and phase offset, etc., thereby providing higher accuracy in a specific network scenario. Several related works focused on developing ray-tracing based channel models [6, 18, 25], such as in [11], the authors studied a Quasi-deterministic (QD) channel model for mmWave networks using ray-tracing technique to generate deterministic components combined with stochastic models for the generation of diffuse components. [2] also

implemented the QD channel model for 802.11ad networks in ns-3 that can interface with the NIST ray tracer [3]. This QD methodology exploiting the deterministic description of the environment has been proposed as a candidate channel modeling approach for IEEE 802.11ay standard [14].

Compared to the statistical channel model, the ray-tracing based model can provide an extremely precise simulation result, but it is more computationally intensive than the statistical model for the generation of a single channel instance, which may limit the usage of large-scale simulations, especially when the density of deployed objects (i.e., reflecting surfaces), client locations, and APs is fairly high in the environment.

In what follows, we first introduce our implementation on a WLAN scenario module and a statistical channel module in ns-3, and then study the network performance provided by our implemented channel and a QD channel with extensive ns-3 simulations.

3 NS-3 IMPLEMENTATION

In this section, we provide an overview of our implementations on obstacle-specific scenario model and sparse cluster-channel model in an 802.11ad ns-3. The source code can be found at [17].

3.1 Obstacle-specific Scenario Model

In the 802.11ad WLAN, due to the susceptibility of 60 GHz mmWave signals to blockages, small changes in the location of communicating devices can have a dramatic impact on link performance. For example, at 60 GHz, when a LoS path between a transmitter and a receiver is blocked by an obstacle, it may lead to 20−30 dB of additional received signal loss. Therefore, accurately modeling obstacles in the environment is critical for mmWave network simulations. On the other hand, with the knowledge of obstacle distribution and tranceivers' positions, LoS/NLoS condition of a mmWave path should be determined based on the accurately geometric calculation instead of a simple probabilistic model, which will make the estimation on channel quality more precise. In this regard, since ns-3 lacks a general way to set up the specific scenario with obstacles in WLAN, we develop a new class `WiFiScenario` under the general `wifi` module. As shown in Figure 1, `WiFiScenario` mainly includes the following classes and functionalities:

Scenario configuration: We provide the room configuration functionality `SetRoomConf()`, which can generate a single rectangular room with arbitrary length and width. Based on our previous work in [13], we also implement the functionality of LoS-optimal ceiling-mounted AP placement for different numbers of APs, such that ns-3 users can easily determine the best AP deployment in the specific scenario by calling `AllocateOptAP()`.

Obstacle generation: We implement the `Obstacle` class that can generate cuboid-based objects to model furniture items in the network scenario. Generally, we provide two generation mode: 1) *random generation modes*, where the center of each obstacle follows a Poisson point process with a specific density λ, the widths, lengths, and heights of furniture-type obstacles follow truncated normal distributions with specific parameters, and each obstacle's orientation follows a uniform distribution from 0 to π; 2) *deterministic generation mode*, where obstacles are generated with specified locations and dimensions that are provided within the simulation

script. The latter mode can be used to create a deterministic WLAN scenario representing a specific office/lab environment having furniture items at known locations.

Client allocation: We implement the `ClientAllocation` class to generate the locations of the client devices. We provide different client placement methods that allow ns-3 users to select locations that follow: (1) the uniform distribution within the room, (2) a truncated normal distribution within a specific area in the scenario, or (3) an obstacle-dependent distribution, where an obstacle is first randomly chosen as the base location, and then the client is uniformly distributed on the top or sides of the selected obstacle.

LoS/NLoS analysis: With the knowledge of the scenario configuration, obstacle sizes and locations, and client locations, a `LoS-Analysis` class is implemented to enable an accurate LoS-determination function. This function checks whether the direct line between an AP and a client intersects any obstacle, and a LoS flag is returned if no intersection exists after traversing all obstacles, otherwise the client is NLoS to that AP.[1]

We also provide the interface `SetScenarioChannel()` to enable the `WifiChannel` module to obtain the LoS/NLoS results of established links from the `WiFiScenario` module, which helps the channel modeling procedure as described in the next subsection.
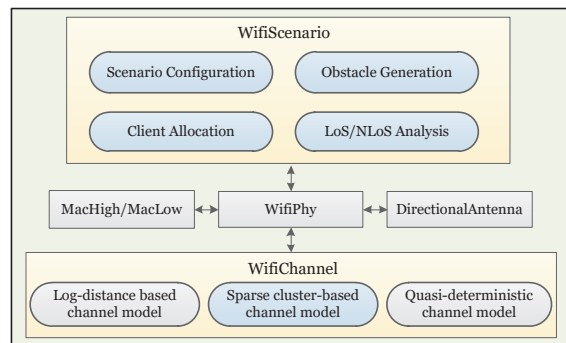

Figure 1: New Added Classes (Marked in Blue Color) in Wi-Fi Module of 802.11ad ns-3

3.2 Sparse Cluster-based Channel Model

We implement the sparse cluster-based (SC) channel based on Saleh-Valenzuela (S-V) model [23] to simulate 60 GHz indoor scenario in ns-3, which characterizes the multipath components (MPCs) arriving in clusters, formed by multiple reflections from the objects in the vicinity of a transceiver. Figure 2 reports a diagram for the procedures involved in the channel model implementation.

In specific, we provide the interface `SwitchSCchannel()` in `WifiScenario` module to toggle between different channel models, such that ns-3 users can flexibly choose different appropriate channel model when they set up the WLAN scenario, where the enabler flag can be transferred to `WifiChannel` module with

---

[1]Note that the ns-3 `Building` module includes a crude LoS estimation, where two nodes in the same building are considered LoS and nodes not in the same building are considered NLoS, whereas our implemented function does a more accurate LoS determination when nodes are located in the same building/room with multiple obstacles deployed. Integration of more accurate LoS determination into the ns-3 `Building` module is future work.
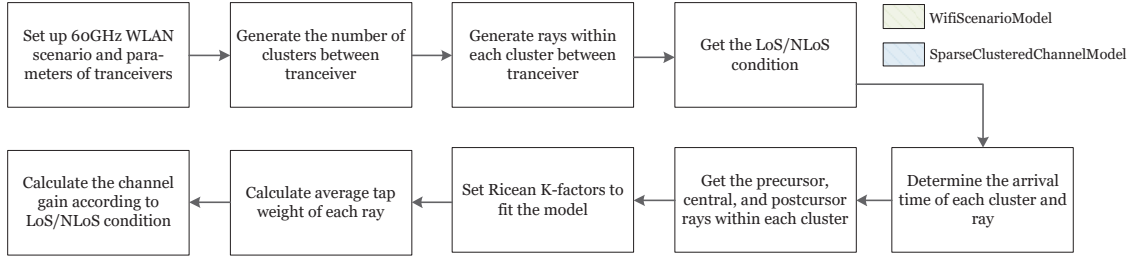
Figure 2: Diagram of the SC Channel Realization Procedure

the interface `SetScenarioModel()`. In SC channel modeling, the LoS component is modeled based on the free-space path loss, and for NLoS components, we generate the clusters l and rays k within each cluster arriving according to Poisson processes with different rates and having inter-arrival times that are exponentially distributed, where the generalized impulse response is derived by following equation as defined in [20]:

$$h(t) = \sum_{l=0}^{L-1} \sum_{k=0}^{N_r-1} a_{k,l} \cdot \exp(j\phi_{k,l}) \cdot \delta(t - T_l - \tau_{k,l}), \quad (1)$$

where the number of clusters L and the number of rays within each cluster N_r are modeled as Poisson distributed with predefined parameter $\bar{L}$ and $\bar{N}_r$, respectively. The phases $\phi_{k,l}$ are uniformly distributed random variables, T_l is the cluster arrival time given by a Poisson process with arrival rate Λ, and the ray arrival time $\tau_{k,l}$ follows two-side exponential decay with mixture the ray arrival rate λ_- and λ_+, i.e.,

$$\begin{cases} P(\tau_{k-1,l}|\tau_{k,l}) = \lambda_- e^{-\lambda_-(\tau_{k,l}-\tau_{k-1,l})}, & k < 0 \\ P(\tau_{k,l}|\tau_{k-1,l}) = \lambda_+ e^{-\lambda_+(\tau_{k,l}-\tau_{k-1,l})}, & k > 0. \end{cases} \quad (2)$$

Note that these distribution parameters are specified depending on the LoS/NLoS condition between the transceiver, thus we should first obtain the channel condition result from `LoSAnalysis()` function in `WiFiScenario` module, and then generate the corresponding modeling parameters of clusters and rays. After that, we calculate the average tap weight (i.e., path power gain) of each ray, where the tap weights $a_{k,l}$ are random variables in Eq. (1), which are distributed according to the small-scale fading distribution, i.e.

$$E\{|a_{k,l}|^2\} = \begin{cases} \Omega_0 e^{-T_l/\Gamma} e^{-\tau_{k,l}/\gamma}, & k = 1 \\ \Omega_0 e^{-T_l/\Gamma} e^{-\tau_{k,l}/\gamma} - K, & k \neq 1 \end{cases} \quad (3)$$

where γ is the decay constant for the two-side exponential decay, Ω_0 is the initial amplitude that depends on the distance between the nodes, and the Ricean factor K is introduced to improve the fit of the model into the experimental data [4], where the relative strength of specular component with respect to precursor or post-cursor components is gauged through K. Next, the SC channel gain between the transmitter and receiver is calculated as $G = \rho + \sum_l \sum_k |a_{k,l}|^2$, where ρ is computed based on Friis propagation loss model, i.e., a function of directional antenna gains, the distances between nodes, the signal wavelength, and the reflectivity of surrounding objects [4, 21]. Specifically, when a LoS condition exists, G is determined by the path gain ρ of the dominant LoS component plus lower-order reflection terms, whereas in NLoS conditions, the total path gain

is composed solely of the path gain of NLoS components with the reflection coefficient R_0, including several clusters and rays that follow the specific distributions. Finally, the received power at RX side is calculated as the sum of transmitted power `txPowerDbm` and G to estimate the received signal-to-noise power ratio performance.

By default, all predefined modeling parameters (e.g., cluster/ray decay time, arrival rate, K-factor, and Ω_0, etc.) are chosen from [4, 23], which are derived based on measurements in real 60 GHz office/lab network environments. Due to the use of narrow-beam directional antennas in 60 GHz WLAN scenarios, the expected number of clusters and rays at each receiver location are set as 2 and 6, respectively, which is in accordance with [15]. In addition, we provide three different reflective coefficient distributions in the channel model, which are all normal distributions: $\mathcal{N}(0.35, 0.05)$ (Mode 1), $\mathcal{N}(0.6, 0.05)$ (Mode 2), and $\mathcal{N}(0.85, 0.05)$ (Mode 3). These are intended to model scenarios with objects having low, medium, and high reflectivity, respectively. We provide the interface `SetReflectMode()` for ns-3 users to select different reflective modes in `WiFiScenario` module, and Mode 2 is set by default in the simulator.

3.3 Quasi-deterministic Channel Model

To simulate the ray tracing-based channel model as a comparison point, we adopt the Quasi-Deterministic (QD) channel model from [2], which determines the geometry-based MPCs by modeling the interaction of the mmWave signal with object surfaces. The MPCs are obtained by ray-tracing techniques, and the channel impulse response is defined in [2] as:

$$h(t) = \sum_{i=0}^{N-1} 10^{-PL_i/20} e^{j\phi_i} \cdot (Y_{rx_i} \cdot Y_{tx_i}) \cdot e^{-j2\pi f t_i}, \quad (4)$$

where N is the number of generated rays, PL_i and ϕ_i are the path loss and phase shift of ray i, and Y_{tx_i} and Y_{rx_i} are the radiation pattern of the transmitter and receiver array at ray i, respectively.

For the evaluation results of QD model in this paper, we directly use the ns-3 802.11ad simulator with QD channel implementation from [2], which is developed jointly by the U.S. National Institute of Standards and Technology (NIST) and the IMDEA Networks Institute. Specifically, we run ns-3 simulations using the QD channel model with the following steps:

(1) A WLAN scenario is set up with multiple objects (i.e., cuboid obstacles) in the room, and valid locations of APs and clients[2].

---

[2] The valid node positions are constrained so that a node is not inside any objects or in conflict with another node's position.
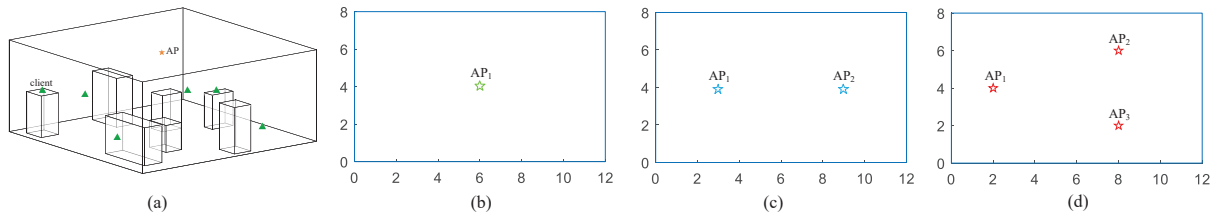
Figure 3: Scenario and AP Deployments: (a) Scenario Example; (b)-(d) Deployments of 1–3 Ceiling-mounted APs

(2) For the given scenario, the QD channel is realized by using NIST QD channel realization software [3], which uses ray tracing within MATLAB® to determine the strongest path components. The software then generates a QD output file that includes the delay, path gain, AoD, and AOA, etc, for the strongest components.

(3) The QD output file is then directly used as input to ns-3 802.11ad QD model, which parses the file and uses Eq. (4) to compute the channel gains.

Note that in our simulated scenarios, the traced MPCs are interacting not only with the walls, ceiling, and floor, but also with the objects deployed in the room, which provides high resolution estimates based on the ray tracing technique.

4 EVALUATIONS AND RESULTS

4.1 Scenario Settings

We consider a room configuration of 12m×8m×3m with the obstacle model of Section 3.1 and the following specific features: 1) obstacles are randomly placed on the floor; 2) the center of each obstacle follows a Poisson point process with a specific density λ (number of obstacles in unit area); 3) the widths, lengths, and heights of obstacles follow the truncated normal distributions W~ $\mathcal{TN}$(0.56, 0.08, 0.25, 1.25), L~ $\mathcal{TN}$(1.08, 0.18, 0.5, 1.75), and H~ $\mathcal{TN}$(1.5, 0.35, 1.2, 2.0)), respectively; 4) each obstacle's orientation follows a uniform distribution $\Theta \sim \mathcal{U}(0, \pi)$. Each client is randomly deployed within the room, and mmWave APs are placed according to the optimal placement methods from [13] (see Figure 3 (b)–(d)). We employ a flat-top directional antenna model with a constant high main lobe gain within a narrow beamwidth and zero gain outside the main beam. This is similar to the directional antenna model used in the QD ray-tracing simulation. This setting is based on a real-life lab environment as a guiding example. All evaluations are done at the mmWave frequency of 60 GHz based on IEEE 802.11ad protocol with single-carrier PHY mode, and all length units are in meters throughout the paper.

In this setting, we evaluate the user throughput performance over different Wi-Fi scenarios based on the SC and QD channel models in ns-3. To perform a comprehensive comparison between the two channel models, we set up various network scenarios with different numbers of deployed APs (1–3 APs), obstacle densities λ (low, medium, and high densities with $\lambda = 0.1/m^2$, $0.2/m^2$, and $0.3/m^2$, respectively), and reflection coefficients (low, medium, and high reflectivities with mean values of 0.35, 0.60, and 0.85, respectively). For each combination of obstacle density, AP deployment, and reflection coefficient, we randomly generate 5 different obstacle configurations using the `WiFiScenario` module. Each data point

in our results is an average value over 100 simulation runs, where there are 20 different randomly located clients simulated over the 5 different obstacle configurations for each set of parameters.

In one run, the randomly located client is allocated a specific time slot for downlink transmission with its connected AP, and the link throughput (Th) under both SC and QD channels is evaluated. We define a performance difference ratio (PDR) to measure the difference between the SC and QD channel models in a simulation run, i.e., $PDR = |Th_{SC} - Th_{QD}|/(Th_{max} - Th_{min})$, where the denominator represents the difference between the maximum throughput and minimum throughput observed across all simulation runs in a data set.[3] Since ns-3 is a packet-level simulator and most users are interested in network-level measurements, we chose to compare packet throughput results rather than PHY-layer metrics such as signal-to-noise ratio.

In addition to comparing the SC and QD channel models' throughputs, we also tune the SC model parameters to better model the different scenarios and we compare the computation times associated with the different calculations in the two models. Note that spatial correlation is accounted for in LoS/NLoS calculations. However, any potential spatial correlation in nearby NLoS channels is not accounted for due to the stochastic nature of the SC model.

4.2 Comparison Between SC and QD Channel Models for Medium Reflectivities

We begin by investigating the PDR for varying numbers of APs and obstacle densities with the reflectivity set to the middle value. First, with the medium obstacle density, we vary the number of deployed APs according to the placement methods shown in Figure 3 (b)-(c). The cumulative distribution function (CDF) plot of PDRs over all simulation instances is reported in Figure 4, and the results of LoS and NLoS cases are shown separately. It is quite clear from the figure that the two different models produce nearly identical throughputs under LoS conditions. When an LoS path between the client and an AP exists, the dominance of the LoS path term in the channel gain produces very similar results for the two models. There is some small variation in the predicted gain for the SC model due to its stochastic nature. This shows up in the single AP case, where a very small percentage of cases show a small but perceptible throughput difference from the QD model. When there are multiple APs, the gain is chosen as the maximum over the paths to the

---

[3]In ns-3's 802.11ad module, the maximum data rate on a link is approximately 4.6 Gbps (corresponding to MCS 12). Since we simulate only a single link at a time to compare the two channel models, we set the application data rate to 4.5 Gbps in order to saturate the highest-quality link simulated. This resulted in a maximum achieved throughput of around 4 Gbps, which is an upper bound on the PDR's denominator.
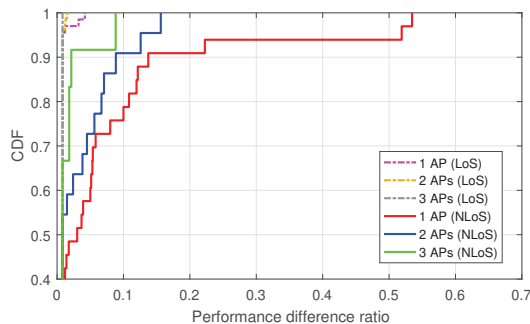
Figure 4: CDF of PDR for LoS and NLoS Links and a Varying Number of APs

Figure 5: CDF of PDR for LoS and NLoS Links and Varying Obstacle Density

different APs, which results in a smaller variation than for a single random channel gain.

From Figure 4, we see that the largest differences between the two models occurs when no LoS path exists to any of the APs. However, even for NLoS cases, 75% or more of the links have a PDR of 0.1 or less. This corresponds to an absolute difference of at most 400 Mbps, which is very close to the average difference between two consecutive MCS levels (data rates) in 802.11ad. Thus, in the vast majority of NLoS cases, the SC model results in a throughput that amounts to at most a difference of one MCS level, which is quite good. We also observe that having multiple APs reduces the difference between the two models substantially, again due to choosing the maximum gain across the different APs.

In Figure 5, we investigate how the obstacle density impacts the performance difference between SC and QD channels with 2 APs deployed. This case shows very similar behavior to the varying APs scenario in that LoS cases show very little difference between the two models while NLoS cases have a larger PDR. We see from the figure that for low and medium obstacle densities, the two models throughputs' are still fairly close for NLoS cases while larger differences occur at high obstacle densitites. This is because with more objects deployed in the scenario, QD channel has more potential to produce better-quality reflection paths that contribute to the link performance, which makes the SC channel model underestimate the channel gain with its fixed statistical modeling parameters.

4.3 Parametric Analysis of SC Channel Model for Medium Reflectivities

By default in the simulator, the expected number of clusters $\bar{L}$ and rays $\bar{N}_r$ within each cluster are set as 2 and 6, respectively, based on the experimental investigations from [15]. Here, still considering the medium reflectivity case, we increase these two parameters to 3 and 8 and evaluate the PDR across different scenario configurations as shown in Figure 6 and Figure 7. Compared to the corresponding results with default parameters in Figure 4 and Figure 5, the PDR is further reduced; for all cases, the throughputs for the two channel models on more than 90% of the NLoS links were within 10% of each other. This result demonstrates that increasing the expected number of clusters and rays in SC channel model can improve the accuracy of the SC model for this medium reflectivity case.
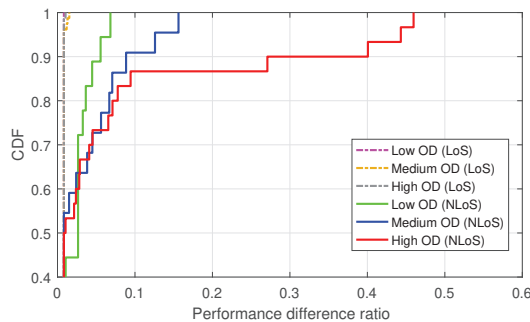
So far, we have looked at comparisons on a per link basis. However, one also might be interested to evaluate performance that is averaged over multiple client locations for a given scenario. For example, considering the worst case with 1-AP and medium obstacle density (see red-solid line in Figure 6), the PDR averaged over 20 client locations for the NLoS links are 0.0432, 0.0355, 0.0265, 0.0146, and 0.0309, for the 5 different obstacle configurations . Thus, the throughput calculated under the SC channel model is within about 1.5–4% of the QD channel model's throughput when averaged over 20 client locations, even for the worst case scenario and only considering the difficult NLoS cases.
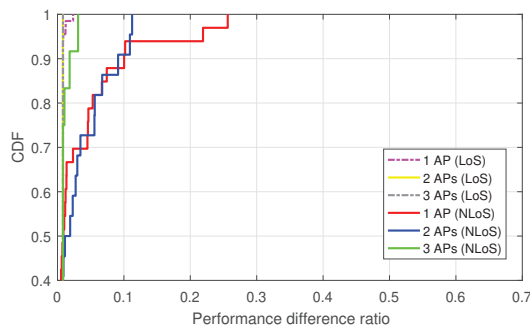

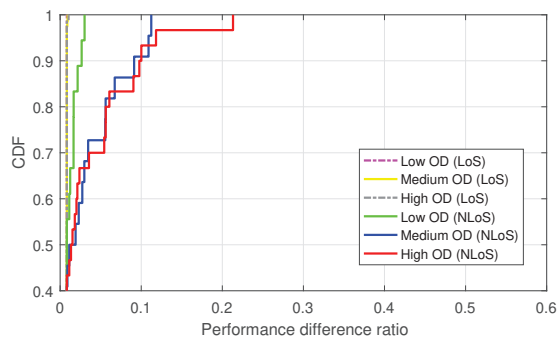**Figure 6: CDF of PDR for Varying Number of APs with Tuned Channel Parameters**

Figure 7: CDF of PDR for Varying Obstacle Density with Tuned Channel Parameters

Next, we perform a detailed study on parametric tuning in SC channel model. Here we choose two scenarios having larger PDRs as reference cases, i.e., the 1-AP scenario in Figure 4 and the high-OD scenario in Figure 5, which are referred to as **Case 1** and **Case 2** for simplicity. Then we tune the SC channel parameters $\bar{L}$ and $\bar{N}_r$ within a larger range to evaluate the performance difference between SC and QD channel.
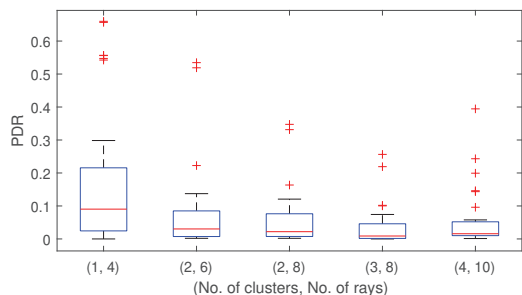

Figure 8: PDR for Different SC Channel Parameters and NLoS Instances Only (Case 1)

Since SC and QD channels show a fairly good consistency under LoS conditions, here we solely focus on the NLoS links. Figure 8 shows the box-plot of PDR under various parameter settings for Case 1. It is clearly observed that the performance difference between two channels becomes smaller when increasing the expected number of clusters and rays, but it is not always true that the larger $(\bar{L}, \bar{N}_r)$ the better PDR, since the optimal point is found at around (3, 8) in the evaluated cases. The same result can be seen in the Figure 9 for Case 2, and tuning $\bar{L}$ and $\bar{N}_r$ to (3, 8) or (4, 10) results in a good performance agreement between the two channel models. Thus, contrary to the results reported in [15], we find that the (2, 6) parameter choices for clusters and rays is *not* the best choice, at least when considering agreement with the ray-tracing-based QD channel model at medium obstacle reflectivity.
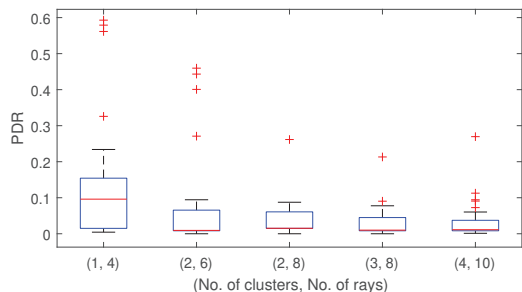

Figure 9: PDR for Different SC Channel Parameters and NLoS Instances Only (Case 2)

4.4 Comparison Between SC and QD Channel Models for Different Reflectivities

In this section, we investigate how the reflectivity of objects impacts the evaluated performance for the two channel models. As discussed in Sec. 3.2, three different reflectivity modes are provided

in the SC channel model, which apply low, medium, and high reflection coefficients. Here we fix $\bar{L}$ and $\bar{N}_r$ at (3, 8), and then vary the reflectivity mode in the evaluated network scenarios.

Figure 10 shows the results of the Case 1 scenario, which was the most problematic for the SC model at medium reflectivity. We can see that the performance difference becomes smaller between the two channel models with the higher reflectivity mode. In that situation, the PDR even for NLoS links is less than 0.08, which is quite good. This is because with objects made of highly reflective materials, e.g. metal, NLoS reflection paths retain more signal power resulting in link throughputs that are close to the maximum achievable rate in 802.11ad WLANs, thereby narrowing the performance gap for the two channel models. At low reflectivity, the performance gap for NLoS links gets slighty larger than at medium reflectivity for this problematic Case 1. In this situation, the QD model consistently predicts very low rates for the NLoS links while the stochastic nature of the SC model produces some higher rates resulting in a somewhat larger PDR.
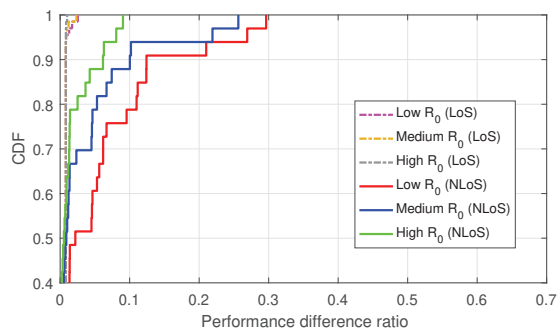

Figure 10: CDF of PDR for Different Reflectivity Scenarios

4.5 Computation Time for SC and QD Channel Models

In this section, we compare the simulation running times[4] for the SC and QD channel models. The SC channel running time is only within ns-3, whereas the QD channel running time includes both the MATLAB® ray-tracer execution time and the ns-3 simulation time. As an additional reference point, we show the running time for the same simulations under the default log-distance-based path loss model. We note that the simple log-distance-based model is known to be highly inaccurate for mmWave channels due to the fact that it ignores the sharp differences between LoS and NLoS links. However, its running time provides a point of reference for the simulation slowdown when using more complex channel models.

Each data point in the figures is the average running time over 5 obstacle configurations where, for each configuration, the cumulative running time over 20 simulation runs with different client locations is calculated. Each simulation run covered 0.5 seconds of network execution, which at the very high application rate of 4.5 Gbps, corresponds to about 200,000 WiFi packets worth of data per simulation run. Figure 11 shows the running times as the number of APs is increased and Figure 12 shows the running time for different

---

[4]We evaluate the running times on an Intel(R) Core(TM) i3-2120 3.30GHz CPU workstation with 2 cores and 3 logical processors.

obstacle densities. As is expected, increasing the number of APs or obstacles slows down the simulations, but the running time with the SC channel model increases much more slowly as the number of APs or the obstacle density increases, as compared to the QD model. While the ns-3 times are fairly similar for the SC and QD models, the MATLAB® ray tracing time for the QD model increases rapidly with the number of APs or obstacles. This is as expected due to the number of rays that must be traced being substantially greater when there are more APs or obstacles to consider.
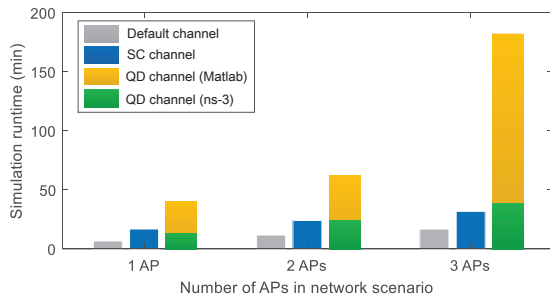

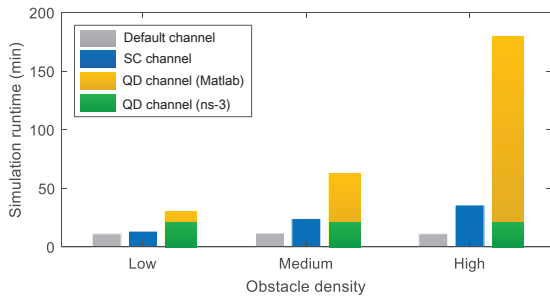**Figure 11: Simulation Running Time vs. Number of APs for Different Channel Models**

Figure 12: Simulation Running Time vs. Obstacle Density for Different Channel Models

When comparing the running time of the SC model simulations to that of the highly inaccurate default model, we see that, in most cases, there is roughly a 2x slowdown. However, for low obstacle densities, the slowdown is very slight while for high obstacle densities, it is closer to a 3x slowdown. Given its substantial increase in accuracy, the SC model slowdown could be considered an acceptable trade-off for all but the most time-sensitive simulations.

5 CONCLUSIONS AND FUTURE WORK

In this paper, we reported on the accuracy and running time of a sparse cluster-based (SC) channel model for mmWave WLAN simulation. While these early results are fairly promising, there are issues still to be addressed. The simulations reported herein involved homogeneous environments where all obstacles (including walls) had the same reflectivities. More study is required to determine how to get the best accuracy from the SC model in heterogeneous environments. However, we believe that modeling only the more highly reflective objects in the environment might still yield fairly accurate results since those will be the dominant scatterers. A challenge on the computational efficiency aspect is how to deal with the necessary LoS calculations when clients are mobile. The simulation results reported herein were for stationary clients

so only one LoS calculation was needed per simulation run. We plan to explore pre-calculated LoS maps and probabilistic LoS modeling to target scenarios with mobile clients.

REFERENCES

[1] 3GPP, "Study on Channel Model for Frequencies from 0.5 to 100 GHz", 2019.

[2] Hany Assasa, Joerg Widmer, Tanguy Ropitault, and Nada Golmie. 2019. "Enhancing the ns-3 IEEE 802.11 ad Model Fidelity: Beam Codebooks, Multi-antenna Beamforming Training, and Quasi-deterministic mmWave Channel", *Proc. of Workshop on ns-3*, Florence, Italy.

[3] Anuraag Bodi, Steve Blandino, Neeraj Varshney, Jiayi Zhang, Tanguy Ropitault, Mattia Lecci, Paolo Testolina, Jian Wang, Chiehping Lai, and Camillo Gentile, "NIST Quasi-deterministic Channel Realization Software Documentation", 2021.

[4] Dajana Cassioli. 2011. "UWB Moves up to mmWaves: A Channel Modeling Perspective", *Proc. of IEEE Int'l Conference on Ultra-Wideband*, Bologna, Italy.

[5] Vittorio Degli-Esposti, Franco Fuschini, Enrico M. Vitucci, Marina Barbiroli, Marco Zoli, Li Tian, Xuefeng Yin, Diego A. Dupleich, Robert Muller, Christian Schneider, and Reiner S. Thoma. 2014. "Ray-tracing-based mm-Wave Beamforming Assessment", *IEEE Access*, vol. 2.

[6] Franco Fuschini, Enrico M. Vitucci, Marina Barbiroli, Gabriele Falciasecca, and Vittorio D. Esposti. 2015. "Ray Tracing Propagation Modeling for Future Small-cell and Indoor Applications: A Review of Current Techniques", *Radio Science*.

[7] IEEE Standard 802.11ad-2012. https://ieeexplore.ieee.org/stamp/stamp.jsp?arnumber=6392842

[8] IEEE Standard 802.11ay/Draft 0.5-2017: *Wireless LAN Medium Access Control (MAC) and Physical Layer (PHY) Specifications— Amendment 7: Enhanced Throughput for Operation in License—Exempt Bands Above 45 GHz*, Aug. 2017.

[9] Leonardo Lanante Jr., Sumit Roy, Scott E. Carpenter, and Sebastien Deronne. 2019. "Improved Abstraction for Clear Channel Assessment in ns-3 802.11 WLAN Model", *Proc. of Workshop on ns-3*, Florence, Italy.

[10] Stephen G. Larew, Timothy A. Thomas, Mark Cudak, and Amitava Ghosh. 2013. "Air Interface Design and Ray Tracing Study for 5G Millimeter Wave Communications", *Proc. of IEEE Globecom Workshops*, Atlanta, GA, USA.

[11] Mattia Lecci, Michele Polese, Chiehping Lai, Jian Wang, Camillo Gentile, Nada Golmie, and Michele Zorzi, "Quasi-deterministic Channel Model for mmWaves: Mathematical Formalization and Validation", *arXiv preprint arXiv:2006.01235*.

[12] Yuchen Liu and Douglas M. Blough. 2019. "Analysis of Blockage Effects on Roadside Relay-assisted mmWave Backhaul Networks", *Proc. of IEEE Int'l Conference on Communications*, Shanghai, China.

[13] Yuchen Liu, Yubing Jian, Raghupathy Sivakumar, and Douglas M. Blough. 2019. "Optimal Access Point Placement for Multi-AP mmWave WLANs", *Proc. of Modeling, Analysis and Simulation of Wireless and Mobile Systems*, Miami, FL, USA.

[14] Alexander Maltsev, Andrey Pudeyev, Artem Lomayev, and Ilya Bolotin. 2016. "Channel Modeling in the Next Generation mmWave Wi-Fi: IEEE 802.11 ay Standard", *Proc. of European Wireless*, Oulu, Finland.

[15] Alexander Maltsev, Roman Maslennikov, Alexey Sevastyanov, Alexey Khoryaev, and Artyom Lomayev. 2009. "Experimental Investigations of 60 GHz WLAN Systems in Office Environment", *IEEE Journal on Selected Areas in Communications*.

[16] Network simulator ns-3, https://www.nsnam.org/

[17] ns-3 802.11ad, https://github.com/yuchen-sh/mmWave-WLAN-802.11ad

[18] Joan Palacios, Danilo De Donno, and Joerg Widmer. 2017. "Tracking mm-Wave Channel Dynamics: Fast Beam Training Strategies under Mobility", *Proc. of IEEE Conference on Computer Communications*, Atlanta, GA, USA.

[19] Natale Patriciello, Sandra Lagen, Biljana Bojovic, and Lorenza Giupponi. 2019. "An E2E Simulator for 5G NR Networks", *Simulation Modelling Practice and Theory*.

[20] Adel A. M. Saleh and Reinaldo A. Valenzuela. 1987. "A Statistical Model for Indoor Multipath Propagation", *IEEE Journal on Selected Areas in Communications*.

[21] Yozo Shoji, Hirokazu Sawada, Chang-Soon Choi, and Hiroyo Ogawa. 2009. "A Modified SV Model Suitable for Line-of-sight Desktop Usage of Millimeter-wave WPAN Systems", *IEEE Transactions on Antennas and Propagation*, vol. 57, no. 10.

[22] Peter F. Smulders. 2009. "Statistical Characterization of 60-GHz Indoor Radio Channels", *IEEE Transactions on Antennas and Propagation*.

[23] Xianyue Wu, Cheng-Xiang Wang, Jian Sun, Jie Huang, Rui Feng, Yang Yang, and Xiaohu Ge. 2017. "60-GHz Millimeter-wave Channel Measurements and Modeling for Indoor Office Environments", *IEEE Transactions on Antennas and Propagation*, vol. 65, no. 4.

[24] Xuefeng Yin, Cen Ling, and Myung-Don Kim. 2015. "Experimental Multipath-cluster Characteristics of 28-GHz Propagation Channel", *IEEE Access*, vol. 3.

[25] Zhengqing Yun and Magdy F. Iskander. 2015. "Ray Tracing for Radio Propagation Modeling: Principles and Applications", *IEEE Access*, vol. 3.